XU, Lei; TANG, Hong; WANG, Shengwei. Adaptive optimal monthly peak building demand limiting strategy based on exploration-exploitation tradeoff. Automation in Construction, 2020, 119: 103349.

https://doi.org/10.1016/j.autcon.2020.103349



# Adaptive Optimal Monthly Peak Building Demand Limiting Strategy Based on Exploration-exploitation Tradeoff

Lei Xu[1], Hong Tang[1], Shengwei Wang[1,*]

[1] Department of Building Services Engineering, The Hong Kong Polytechnic University, Kowloon, Hong Kong

## Abstract

Peak demand limiting is an efficient means to reduce the monthly electricity cost in cases where peak demand charge is a major factor. This paper presents an adaptive optimal monthly peak building demand limiting strategy based on exploration and exploitation tradeoff in threshold resetting. Two basis function components are developed, including a building load prediction model and an optimal threshold resetting scheme. The building load prediction model is built using the artificial neural network (ANN). The optimal threshold resetting scheme is developed based on the cost-benefit analysis, and the predicted building demands and/or actual building power uses. Three basic exploration-exploitation tradeoff schemes (i.e., the non-greedy, the greedy and the ε-greedy schemes) are proposed for optimal threshold resetting. Monte Carlo simulation is conducted to analyze the impacts of the exploration-exploitation tradeoff scheme parameter on the demand limiting performance under uncertainties. The model validation results show that the ANN building load prediction model can achieve satisfactory accuracy with the average mean absolute percentage error (MAPE) of 5.7%. Case studies are conducted and the results show that the strategy based on the three proposed schemes can effectively reduce the monthly peak demand cost in different seasons. Monte Carlo simulation results show that the ε-greedy scheme could achieve higher monthly net cost saving with better robustness when a large value of ε is used in both winter and summer.

**Keywords:** building demand management, ANN model, peak demand limiting, optimal threshold resetting, exploration-exploitation tradeoff.

Corresponding author, email: beswwang@polyu.edu.hk

## 1. Introduction

Buildings, as the largest electricity consumer at the demand side, consume over 40% of overall energy [1] and even over 90% of total electricity consumption in high-density urban areas like Hong Kong [2]. The large energy consumption in buildings poses a great challenge for governments and practitioners to achieve energy reduction and carbon dioxide reduction. Besides, peak building demand (load) is another significant issue which results in huge investment in the power grid development and reduces the grid efficiency. J. Wells et al. [3] estimated that the capacity to meet peak demands during the top 100 h in a year accounted for nearly 20% of the entire electricity cost. This is because the generation and transmission capacities of power grids have to be provided to meet these peak demands that occur occasionally [4]. Tackling with these two issues (i.e., large building energy consumption and huge peak building demand), utility companies (e.g., in Hong Kong) usually charge the monthly electricity bills of buildings based on these two parts. Although different price structures (including these two parts) are applied in different regions, the monthly peak demand cost of a commercial building always accounts for a significant part of the monthly electricity bill due to the high peak demand charge [5]. J. Seem reported that the monthly peak demand cost of a commercial building contributed a considerable part to the monthly electricity bill, sometimes even exceeding 50% in the US [5], and it is typically above 30% in Hong Kong according to the field survey of the authors. Under these price structures, peak demand reduction could contribute to the significant reduction of the electricity cost over a billing period (e.g., a month). Therefore, the development of an effective building demand limiting strategy becomes increasingly attractive for reducing the monthly peak demand and the monthly electricity cost.

To reduce the monthly peak demand cost for commercial or non-residential buildings, many demand limiting control strategies have been developed and applied for the HVAC (heating, ventilation and air conditioning) systems, since a major part of the energy in commercial/non-residential buildings is consumed by the HVAC systems [6,7]. These control strategies involve three main types of used technologies: building thermal mass only, active storage facilities only, and both building thermal mass and active storages, which are elaborated as follows.

For demand limiting using building thermal mass only, P. Xu et al. [8] employed an indoor room temperature resetting strategy in a site study to reduce the daily peak demand in a medium-weight

building. This strategy involves maintaining zone temperatures at the lower comfort limit during the off-peak time and resetting zone temperatures to the upper thermal comfort limit during the on-peak time. K. Lee et al. [9] used three different methods to estimate the set-point trajectories which affect the discharged cooling in building thermal mass for reducing the daily peak thermal load.

With regard to demand limiting using active storage facilities only, G. Henze et al. [10] developed a predictive optimal controller for the ice storage system based on the predictive load and weather information. Results showed that significant daily electricity cost savings could be achieved under the real-time electricity tariff. K. Drees et al. [11] also proposed a rule-based control strategy, which integrates the storage-priority and chiller-priority strategies. The strategy could be easily implemented as it only requires measurements of the building cooling load, building electrical usage and the state-of-charge of the ice storage.

In terms of the combined use of the building thermal mass and the active storage facilities, G. Henze [12] conducted site investigation on the operation cost savings and energy consumption in the combined usage of building thermal mass and active thermal storage under the Time-of-Use electricity tariff. G. Zhou et al. [13] also conducted para- metric analysis to investigate the effects of building mass, utility rate, thermal comfort, central plant capabilities and economizer on the cost saving performance of demand limiting control using the building thermal mass and active thermal storage.

However, most of these control strategies are used and optimized for demand limiting over a short period, e.g., one day. Therefore, these studies might not achieve the maximum cost saving due to the fact that the effective peak demand used for electricity charge calculation is usually the peak over a billing period (e.g., a month) rather than the peak on one day, and some of the limiting efforts would be wasted if the limiting controls are conducted on daily basis.

Compared to the short-term peak demand limiting, monthly peak demand limiting is more difficult due to the fact that there exists greater uncertainty to predict the monthly peak demand of buildings, especially for a single building. The uncertain monthly peak demand would result in the identification of an uncertain limiting threshold when only one static limiting threshold is used for demand limiting control. One of the existing major challenges is how to identify the optimal or practically effective and doable demand limiting threshold over a month. To date, there are very

few studies on monthly peak demand limiting. Y. Sun et al. [14] proposed a demand limiting strategy for maximizing monthly cost savings of commercial buildings, which identified a proper monthly limiting threshold and adjusted the indoor room temperature set-point to restrain the daily peak demand. But this strategy adopted a simple polynomial equation to predict the monthly peak demand, which ignores the great uncertainty of the monthly peak demand. Instead, L. Xu et al. [15] employed an adaptive mechanism in optimal threshold identification/resetting for monthly peak demand limiting considering load uncertainty, which employed the real-time probabilistic weather forecasts in Hong Kong to predict and update uncertain building loads for optimal threshold resetting. But this approach has its own limitation that it aims for a single non-residential building with uncertain peak loads and is only doable when the real-time probabilistic weather forecasts are available, which prohibits its wide application in other building types and other regions without the real-time probabilistic weather forecasts. Therefore, an easy-to-use threshold resetting scheme in an adaptive mechanism is needed for building peak demand limiting over a month.

Normally, an adaptive threshold resetting scheme for peak demand limiting is based on the updated building load predictions, which can be obtained from a building load model and real-time weather forecasts (e.g., 9 days ahead in Hong Kong). But this approach still might not guarantee to identify the optimal limiting threshold over a month. Actually, the ever-changing actual power uses from the first day to the current day can be also useful to identify/update an adaptive and doable limiting threshold, which could achieve a considerable monthly bill saving but is seldom considered in existing monthly demand limiting strategies. No existing study has even considered the tradeoff between using the updated building load predictions and the ever- changing actual power uses for threshold resetting for peak demand limiting over a month.

This tradeoff between using load predictions and actual power uses reflects the fundamental tradeoff in most learning problems: exploration vs. exploitation. The exploration-exploitation trade-off is at the heart of any sequential decision-making process in uncertain environments [16]. This trade-off characterizes the balance between achieving benefits from a known solution (could be non-optimal) and continuing to search in hope for better solutions [17]. The typical learning problem for exploration and exploitation tradeoff is the multi-armed bandit (MAB) issue [18]. MAB considers independent arms, each providing a random contribution (benefit) according to its own distribution. A decision maker, unknown of these distributions, chooses one arm at each time step and tries to maximize the entire expected contribution. The decision maker should decide

whether to explore arms to learn unknown information or exploit the current known information by selecting the arm with the highest contribution. When applying the concept of MAB framework to adaptive limiting threshold resetting over a month, each day can be viewed as an arm. The proper limiting threshold can be determined and updated on the basis of building load predictions or the ever-changing actual power uses, which can be viewed as an example of how to explore new information or exploit known information for a best choice, respectively.

This research, therefore, aims to develop an adaptive monthly peak demand limiting strategy for buildings based on exploration-exploitation tradeoff between using load predictions and actual power uses. Compared with the existing monthly demand limiting strategies for individual buildings, the proposed strategy and this study have the following main novelty and original contributions.

- A new adaptive monthly peak building demand limiting strategy is developed based on the tradeoff between exploring the real-time median-term building load predictions and exploiting ever-changing actual power uses over a month. This strategy can be easily and widely applicable in monthly peak demand limiting for a single building or building clusters.
- Three exploration-exploitation tradeoff schemes for threshold resetting are developed and validated on the basis of real data of an educational building in different seasons.
- The impacts of the exploration-exploitation tradeoff scheme parameter (i.e., the weight for tradeoff) on the uncertain demand limiting performance over a month are comprehensively considered.

In this study, three exploration-exploitation tradeoff schemes are applied to reset the optimal limiting threshold over a month. ANN (artificial neural network) is adopted to establish the building load prediction model. Five years of electricity load data in an educational building in Hong Kong are used to train and validate the proposed building model. Real-time simulation tests are conducted to validate the developed demand limiting strategy. This paper presents the building load prediction model, the optimal limiting threshold resetting scheme, model training and validation results as well as the results of the real-time validation tests.

## 2. Adaptive monthly demand limiting strategy

### 2.1. Overall strategy of adaptive monthly peak demand limiting

The basic approach of the developed adaptive monthly peak demand limiting strategy for an

individual building is shown in Fig. 1. It comprises the building load prediction model, the optimal threshold resetting scheme, and the demand limiting control. The building load prediction model predicts the demand profile based on the online weather forecasts, etc. The optimal threshold resetting scheme identifies the optimal demand limiting threshold based on the predicted demand profiles and/or the measured power uses. The optimal limiting threshold is used for demand limiting through controlling operation of building energy systems (e.g., HVAC systems and/or thermal energy storages). The monthly peak demand limiting strategy works in an adaptive manner in the billing period of a month and starts again in a new billing period.

In this study, the developed optimal threshold resetting determines and continuously updates the optimal limiting threshold. Three basic exploration-exploitation tradeoff schemes for threshold resetting are introduced and compared. The building load prediction model and the optimal threshold resetting scheme are introduced in the following subsections. As there are many studies and methods on the use of HVAC systems and/or thermal energy storages for reducing building peak demands, the system and actual control are not the focus of this study. Instead, an ideal active thermal storage with ideal control is used in the validation tests of the monthly peak building demand limiting strategy in the case studies. Additionally, the indoor thermal comfort using active thermal storage is well maintained since the thermal storage only shifts the corresponding HVAC energy consumption during demand limiting periods.

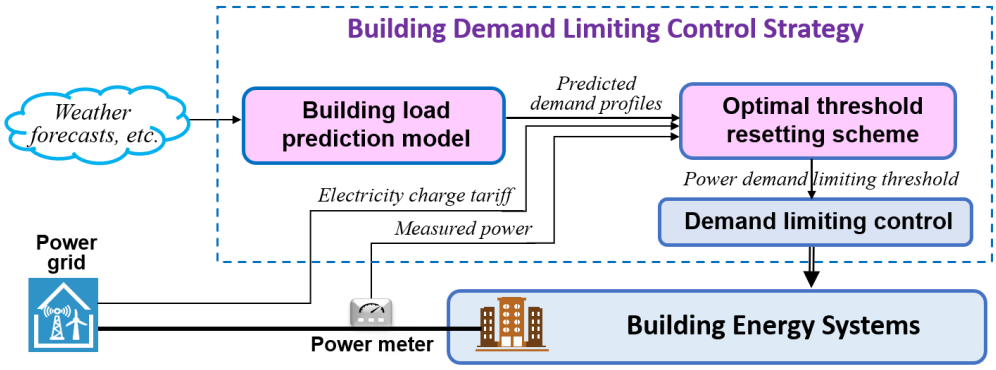


Fig. 1. Basic approach of developed adaptive monthly peak demand limiting strategy

## 2.2. Building load prediction model

The dominant factors for electricity consumption in commercial buildings are outdoor weather conditions and space usage. Traditionally, physical models are established between weather variables and the building load to reasonably predict building energy usages. To achieve better

prediction accuracy, black models (based on data-driven techniques) are applied considering not only the outdoor weather conditions but also the space usage, which is potentially reflected by the calendar information. In this study, ANN, a common data-driven method, is adopted to model the effects of outdoor weather variables and calendar variables on the building load. Two of various weather variables (i.e., outdoor dry bulb temperature and relative humidity) are selected due to their high correlation with the commercial building load in Hong Kong. The solar radiation is less correlated to the load and excluded mainly due to the mutual shading between the high-density buildings in Hong Kong. Besides, three calendar variables (i.e., hour of the day, day of the week, and month of the year) are selected, because the calendar information can potentially reflect the schedules of building functioning and occupant behavior. The internal gain of a building also contributes to electricity consumption and is mainly determined by how the building functions; hence, it also can be reflected by the calendar information.

*2.2.1. ANN modelling*

The ANN is a universal functional approximator and a self-adaptive machine learning method with few priori assumptions [19]. There are different types of neural networks, among which BP (back-propagation) neural network is one of the most popular one [20]. It employs the gradient method to change the weight values and bias values quickly to reduce errors. The typical BP neural network comprises three layers, the input layer, the hidden layer, and the output layer. Moreover, BP neural network contains many learning algorithms. Among these algorithms, the LM (Levenberg-Marquardt) learning algorithm gains much popularity due to its high computational speed in the convergence of the network training and the facts that it offers a better learning process and is one of the most widely applied algorithms [21]. Hence, this study employs the three-layer BP neural network embedded with the LM learning algorithm to train the building load prediction model, as shown in Fig. 2. The detailed ANN model settings are described as follows.

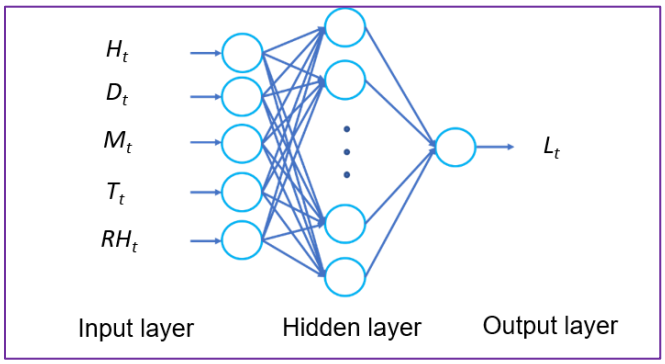

Fig. 2. ANN architecture for the developed building load prediction model.

*Input layer:* The input layer comprises the calendar variables (i.e., hour of the day ($H_t$), day of the week ($D_t$), and month of the year ($M_t$)) and the weather variables (i.e., outdoor dry-bulb temperature ($T_t$), and relative humidity ($RH_t$)). Each calendar variable has certain ranges ($H_t$ =9, 10, …, 20, $D_t$ =1, 2, …, 6, and $M_t$ =1, 2, …, 12), due to the fact that only office hours are considered for load prediction and demand limiting control in this study.

*Hidden layer:* In the hidden layer, the number of hidden neurons determines how well a problem can be learned using BP neural network. In general, an empirical formula could be used to determine the number of hidden neurons [22], as given by Eq. (1). Where, the training pattern represents the correct output [22].

$$m = \frac{1}{2}(\text{inputs} + \text{outputs}) + \sqrt{\text{training patterns}} \tag{1}$$

*Output layer:* The output layer only contains one variable, the building load ($L_t$).

The training and testing samples of the proposed ANN model are deployed with 4/5 and 1/5 of the historical datasets of the input and output variables, respectively. Additionally, both training and validation of the ANN model are built in the MATLAB environment using the Neural Network Toolbox.

*2.2.2. Model parameter identification*

The steepest descent training algorithm is used to tune the weights and biases of the network (i.e., model parameters) to optimize the network performance [23] based on the preprocessed training data. This algorithm minimizes the mean square error (mse) between the network outputs and the target outputs/training data, as given by Eq. (2). Where, $\boldsymbol{Y}^a$ is the actual target output vector. $\boldsymbol{Y}$ is the network output vector.

$$mse = \frac{1}{N}\sum_{i=1}^{N}(\boldsymbol{Y}_i^a - \boldsymbol{Y}_i)^2 \tag{2}$$

Before model parameter identification, the preprocessed training data are obtained by normalizing the raw data using Eq. (3), which helps reduce data redundancy and improve data integrity. Where, $\mathbf{z}$ is a variable.$\mathbf{z}_i$ is a random value of the variable $\mathbf{z}$. $\mathbf{z}_{noz,i}$ is the normalized value. max($\mathbf{z}$) and min($\mathbf{z}$) are the maximum and minimum values in the dataset respectively.

$$\boldsymbol{z}_{noz,i} = \frac{\boldsymbol{z}_i - \min(\boldsymbol{z})}{\max(\boldsymbol{z}) - \min(\boldsymbol{z})} \tag{3}$$

After the proposed ANN model is trained and validated with satisfactory accuracy, the ANN model is used to predict the K days ahead building loads based on the K-day weather forecast duration (K=9 in this study for current applications in Hong Kong).

### 2.3. Optimal threshold resetting scheme

In the optimal threshold resetting scheme, three different control schemes for peak demand limiting are developed according to the building load predictions and/or actual power uses. These schemes are validated and compared in the later case study.

#### *2.3.1. Non-greedy scheme*

The first one is the 'non-greedy scheme' that explores the predicted information without exploiting the known information. In this scheme, the optimal demand limiting threshold is determined/reset on the basis of the predicted K days ahead building demand profile (i.e., merely explore the predicted loads for threshold resetting) on each day (before office hour, e.g., 9:00 AM) in a month. With the optimized threshold, the ideal control of the thermal energy storage is conducted during the on-peak time, by discharging cooling energy when the real-time demand exceeds the threshold. Meanwhile during the off-peak time, the storage is assumed to be fully charged. The net reduction of electrical energy consumption of an entire demand limiting event is assumed as 0, considering the fact that there is usually a rebound after the demand limiting or energy loss using TES, which offsets the reduction of energy consumption [15].

The effects of threshold reset on peak demand, limiting effort and total cost savings in a medium period (e.g., a week) are illustrated in Fig. 3. It can be seen that the total cost saving can reach the maximum value when an optimal limiting threshold ($PD_{set,opt}$) is adopted. In the non-greedy scheme, the total cost saving ($CS_{tot}$) of demand limiting using a particular threshold ($PD_{set}$) in the future K days is estimated on the basis of the predicted K-day demand profile. Eq. (4) shows that the total cost saving is determined by the cost saving of reduced peak demand ($PD_{max}$ - $PD_{set}$) and the cost of limiting effort (i.e., thermal energy consumption $\Delta E_d$). The thermal energy consumption from the thermal storage is assumed proportional (with the coefficient $\lambda$) to the overall COP of the air-conditioning system. In this case, the unit price of limiting effort using thermal storage is also assumed proportional (with the value of $\lambda^{-1}$) to the unit price of electrical energy consumption. Based on the quantified cost savings using different limiting thresholds, the optimal limiting threshold ($PD_{set,opt}$) is determined by maximizing the total cost saving, as given by Eq. (5).

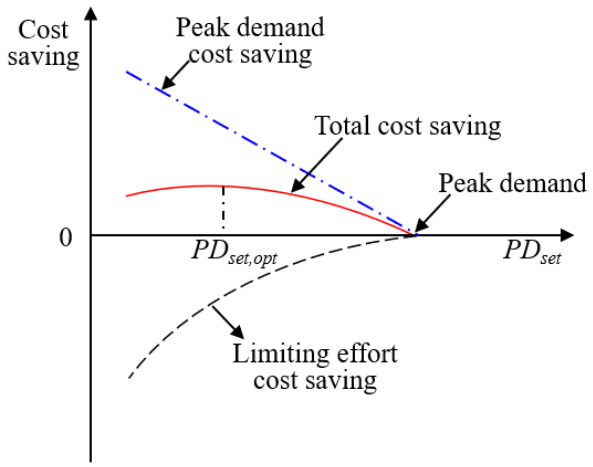


Fig. 3. Effects of threshold reset on peak demand, limiting effort and total cost savings.

$$CS_{tot} = \alpha \times (PD_{max} - PD_{set}) - \beta \times \sum_{d=1}^{K} \Delta E_d \ \ (\Delta E_d \leq Cap) \quad (4)$$

$$PD_{set,opt} = \max_{\forall\, PD_{set}}{}^{-1}(CS_{tot}) \quad (5)$$

Where, $CS_{tot}$ is the total cost saving of demand limiting control in the future K days when a particular limiting threshold is used. $PD_{max}$ is the predicted peak demand in the future K days. $PD_{set}$ is a particular limiting threshold for demand limiting control in the future K days, with a range [$0.5PD_{max}$, $PD_{max}$]. *Cap* is the demand limiting capacity of an active thermal storage. $\Delta E_d$ is the daily thermal energy consumption during the demand limiting period on the future *d*th day, which should be less than the adopted storage capacity. $\alpha$ is the unit price of the electricity demand. $\beta$ is the unit price of demand limiting effort using an active thermal storage, which is taken as the unit price of electrical energy consumption multiplied by $\lambda^{-1}$. $PD_{set,opt}$ is the optimal limiting threshold based on the K-day ahead demand profiles, which should be no less than the actual peak power use up to the moment of decision-making. $max^{-1}$ is the inverse function for computing the maximum value among a set of data. Different to the cost saving function of monthly peak demand limiting in [14], in this study the predicted peak demand in the cost saving function (i.e., Eq. (4)) is adaptive to the K days ahead weather forecasts, which is essential in identifying the adaptive optimal threshold in the non-greedy scheme.

*2.3.2. Greedy scheme*

The second one is the 'greedy scheme' that merely exploits the known information. In this scheme, the optimal demand limiting threshold is determined/reset on the basis of the ever-changing actual power uses from the first day to the current day of a month (i.e., merely exploit the known power

uses for threshold resetting). The control of the thermal storage in this scheme is the same as that in the non-greedy scheme.

In this scheme, the total cost saving ($\widetilde{CS}_{tot}$) of demand limiting using a particular threshold ($\widetilde{PD}_{set}$) is estimated according to the actual power uses during the past *N* days, as given by Eq (6). The optimal limiting threshold ($\widetilde{PD}_{set,opt}$) can be determined by maximizing the total cost saving, like Eq. (5). The number *N* becomes larger, the identified optimal threshold becomes more optimal and effective.

$$\widetilde{CS}_{tot} = \alpha \times \left(\widetilde{PD}_{max} - \widetilde{PD}_{set}\right) - \beta \times \sum_{\tilde{d}=-N}^{0} \Delta\tilde{E}_{\tilde{d}} \ \ (\Delta\tilde{E}_{\tilde{d}} \le Cap) \tag{6}$$

Where, $\widetilde{PD}_{max}$ is the maximum demand in the past *N* days. *N* is the number of days from the first day to the current day of a month (excluding the current day). $\Delta\tilde{E}_{\tilde{d}}$ is daily thermal energy consumption during the demand limiting period on the past $\tilde{d}$th day, which should be less than the storage capacity (*Cap*). $\widetilde{PD}_{set,opt}$ is identified optimal limiting threshold based on the actual power uses, which should be no less than the actual peak power use up to the moment of decision-making. According to the demand management study in [14], a building model (i.e., simplified physical model) [24] can be and is used to estimate the original hourly power use without implementing demand limiting control, based on the actual hourly power use in the condition with the implementation of the demand limiting control.

*2.3.3. ε-greedy scheme*

The third one is the 'ε-greedy scheme' that both explores the predicted information and exploits the known information. In this scheme, the optimal demand limiting threshold is determined/reset on the basis of the tradeoff between the non-greedy scheme and the greedy scheme. The control of the thermal storage in this scheme is the same as that in the non-greedy scheme.

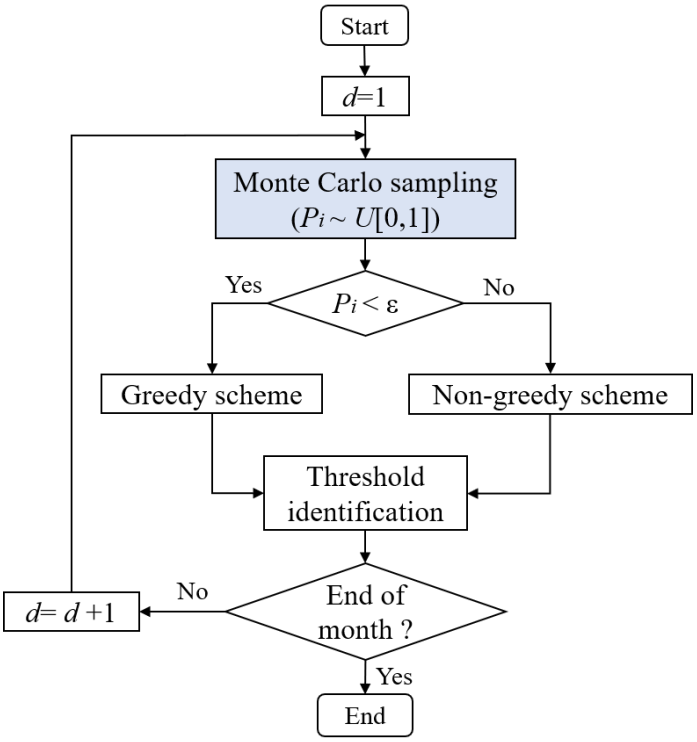


Fig. 4. Flowchart of threshold resetting using the $\varepsilon$-greedy scheme on each day of a month.

This scheme employs a particular probability ($\varepsilon$) to select the greedy scheme to identify $\widetilde{PD}_{set,opt}$ on each day (otherwise, employs the non-greedy scheme to identify $PD_{set,opt}$ with a probability of 1- $\varepsilon$), as illustrated in Fig. 4. It can be seen that on each day (before office hour), the Monte Carlo sampling based on the uniform distribution ($U$[0,1]) is used to generate a random probability ($P_i$), which determines the selection of the greedy scheme when it is less than $\varepsilon$, and vice versa. It is worth noticing that the range of $\varepsilon$ is [0,1], and the $\varepsilon$-greedy scheme changes to the non-greedy scheme when $\varepsilon$ takes 1 and the greedy scheme when $\varepsilon$ takes 0.

## 3. Training and validation of building load prediction model

### 3.1. Description of the building and data

An educational building named Hotel ICON, in The Hong Kong Polytechnic University (in Hong Kong within sub-tropic climate zone), is selected in the study. It is equipped with different research facilities, resource centers, classrooms, and faculty and administration offices. In Hong Kong, the peak demand of commercial/nonresidential buildings usually occurs during the on-peak time (i.e., from 9:00 AM to 21:00 PM, excluding Sundays and public holidays). Peak demand limiting is a critical issue and could contribute significantly to the monthly electricity cost saving. The datasets

of the building load/demand and weather variables only during the on-peak time are used for model training and validation tests, and case studies. The load spikes from chillers' starting in the morning before 8:00 AM are not considered in this study. This choice is also largely due to the fact that these load spikes are not the effective causes of actual monthly peak loads based on analyzing the practical load profiles of many buildings.

In the training and validation tests, the historical data of the load, weather variables, and calendar variables were collected at the hourly time interval from Jan 2012 to Dec 2016. The building electric load profile of Hotel ICON shows a seasonal variation and peak demands in each month, as illustrated in Fig. 5.

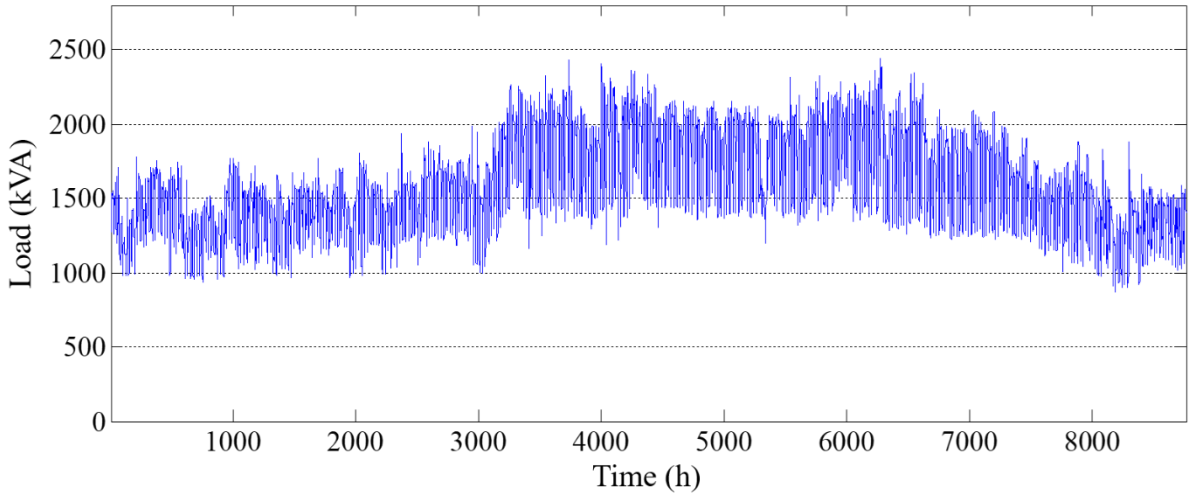


Fig. 5. The building electric load profile of Hotel ICON in 2014

3.2. Model training and results

In the training of ANN model, the historical datasets of the load, weather variables, and calendar variables from Jan 2012 to Dec 2015 were used. The number of hidden neurons in the hidden layer was set as 12 according to Eq. (1) and the trial and error. Besides, the mean square error was set as 0.001, the learning rate was set as 0.5, and the iteration times were set as 1000. The identified weight values and the bias values of the ANN model are listed in Table A.1 of Appendix A.

3.3. Model validation and results

To evaluate the building load prediction model, the commonly used mean absolute percentage error (MAPE) indicator, mean absolute error (MAE) indicator, and root mean squared error (RMSE) indicator are used in this study, as given by Eqs. (7-9). Where, $L_i$ is the measured load

(kVA). $\hat{L}_i$ is the predicted load (kVA). $i$ is a certain number. $n$ is the length of the test time series.

$$\text{MAPE} = \frac{1}{n}\sum_{i=1}^{n}\left|\frac{L_i-\hat{L}_i}{L_i}\right| \quad (7)$$

$$\text{MAE} = \frac{1}{n}\sum_{i=1}^{n}\left|L_i-\hat{L}_i\right| \quad (8)$$

$$\text{RMSE} = \sqrt{\frac{1}{n}\sum_{i=1}^{n}(L_i-\hat{L}_i)^2} \quad (9)$$

In the validation of the ANN model, the historical datasets of the load, weather variables, and calendar variables in 2016 were used. The calculated monthly MAPEs, MAEs, and RMSEs of the test results are listed in Table 1. The average MAPE, MAE, and RMSE were 5.7%, 95 kVA, and 121 kVA in the year, respectively. The minimum MAPE was 4.2%, which occurred in December, and the minimum MAE and RMSE were 60 kVA and 72 kVA, respectively, which occurred in December as well. The validation test results show the prediction accuracy of the developed ANN model is satisfactory.

Table 1. MAPEs and MAEs of validation test results of the developed ANN model in 2016

| Performance metric | Jan | Feb | Mar | Apr | May | Jun | Jul | Aug | Sept | Oct | Nov | Dec |
|---|---|---|---|---|---|---|---|---|---|---|---|---|
| MAPE (%) | 4.4 | 4.9 | 4.6 | 8.1 | 8.7 | 6.0 | 4.9 | 6.0 | 4.4 | 6.0 | 6.1 | 4.2 |
| MAE (kVA) | 66 | 76 | 69 | 123 | 149 | 113 | 93 | 111 | 82 | 104 | 96 | 60 |
| RMSE (kVA) | 108 | 101 | 88 | 147 | 173 | 143 | 114 | 142 | 105 | 140 | 117 | 72 |

The load forecasts and the actual load measurements were compared during office hours in typical summer and winter months (i.e., July and December 2016), as shown in Fig. 6. It can be seen that most load forecasts in these two typical months matched the actual loads with satisfactory agreement. The slight overestimation in both months could result from that some parts of the test sample were not well presented in the training dataset, as shown in Figs. B.1 and B.2 of Appendix B. And the reason could be the system operation change of the hotel complex building in 2016. In principle, a well-trained ANN model is based on the overall performance metrics (e.g. mse), regardless of the frequency of positive/negative absolute errors (randomly derived in both training and testing processes). This slight overestimation (i.e. high frequency of positive errors) was not an issue for that the validation performances were satisfactory, and it could be alleviated by enlarging the model training dataset or using the moving window technique. The extreme peak

load occurred in December, which was beyond the capability of the developed building model. But this would not affect peak demand limiting when a relatively large limiting capacity was employed for demand limiting control.

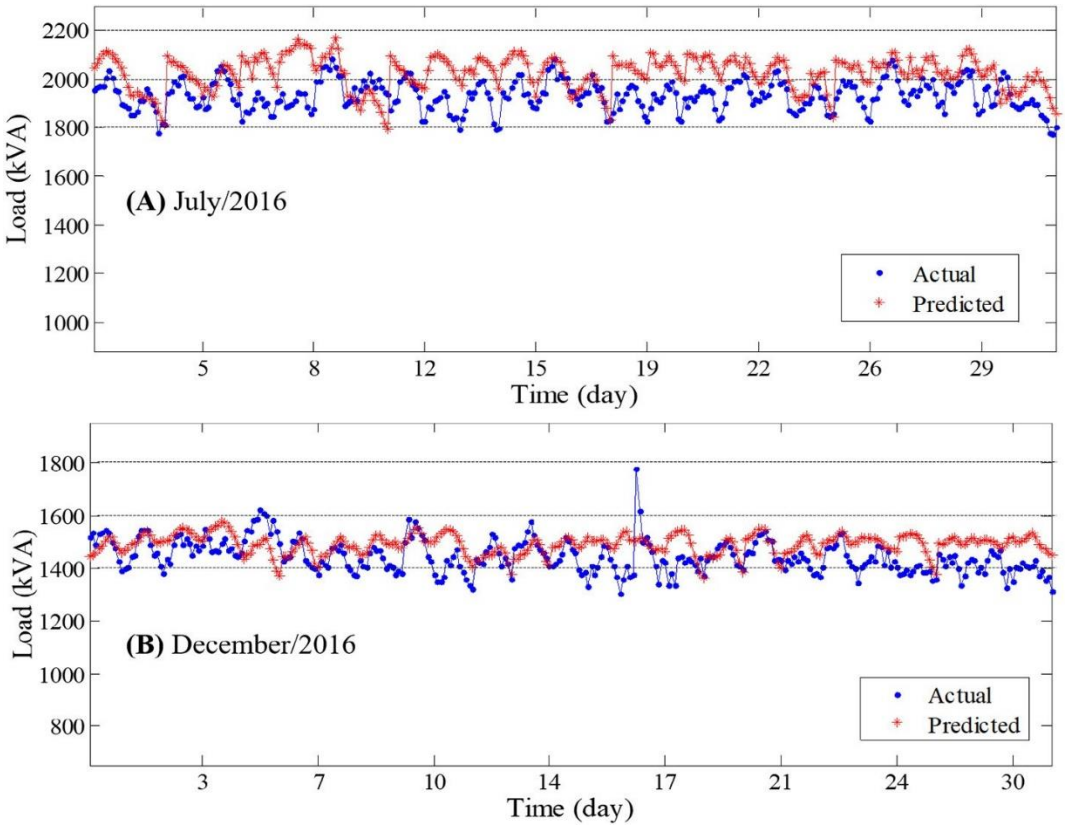


Fig. 6. Load forecasts using the developed ANN model compared with actual load measurements during office hours in two months.

## 4. Case study and test results

Based on the above validated ANN model, two typical months in winter and summer (i.e., Dec/2017 and Jun/2018) are selected for testing the developed adaptive optimal peak demand limiting strategy. In these two months, the 9-day weather forecast data reported daily by the Hong Kong Observatory (HKO) are recorded daily. Moreover, in each month, the three proposed exploration-exploitation tradeoff schemes for threshold resetting are applied and tested.

### 4.1. Identification of parameters in the optimal threshold resetting scheme

To apply the proposed threshold resetting scheme, some parameters concerning the cost saving of demand limiting are identified as follows. The unit price of the electricity demand (i.e., $\alpha$ in equations (4) and (6)) is set as 132 HKD/kVA and the unit price of the electricity consumption is

0.72 HKD/kWh, according to a real tariff from the Hong Kong CLP power company. The unit price of the demand limiting effort using the ideal thermal storage (i.e., $\beta$ in equations (4) and (6)) is calculated as 0.29 HKD/kWh, when assuming that the overall COP of the air-conditioning system is 2.5 earlier [25]. A simplified cold active storage model [26] is used to quantify the demand limiting capacity for the Hotel ICON building and a rather small active storage with the limiting capacity (*Cap*) of 2250 kWh is adopted.

### 4.2. Winter case study and test results

In the winter case study, the datasets during office hours in Dec/2017 are used to validate the adaptive monthly demand limiting strategy using three proposed schemes.

#### *4.2.1. Validation of non-greedy scheme*

In validation of the non-greedy scheme, the 9-day weather forecast data reported/updated daily by the HKO in December are recorded and used to predict 9-day demand profile on each workday (before office hour, i.e., 9:00 AM). Afterwards, the daily updated 9-day demand profile is used to identify/update the optimal limiting threshold according to equations (4-5).

Fig. 7(A) shows the building demand profile of the Hotel ICON building without implementing demand limiting, measured in Dec/2017. It can be seen the monthly peak demand occurred on the fifteenth workday. Two adaptive thresholds are also included. One is the non-greedy adaptive optimal threshold, and the other is the non-greedy adaptive threshold without considering previous peak power use.

Fig. 7(B) shows the power demand profile when implementing demand limiting using the developed demand limiting strategy with the non-greedy scheme. On the first workday, the non-greedy adaptive optimal threshold was determined by conducting cost-benefit analysis of the predicted building demand profile (using equations (4-5)) only. From the second workday, the threshold was updated not only according to the updated building demand profile but also no less than the previous peak power use.

Fig. 7(C) shows the demand reduction when implementing the developed strategy with the non-greedy scheme. During the demand limiting periods, the active thermal storage was discharged to restrict peak demands over the non-greedy adaptive optimal threshold. After implementing demand limiting based on the non-greedy scheme in Dec/2017, the achieved monthly peak demand reduction was 157 kVA (with the accumulated limiting effort of 9,462 kWh), 9.6% of the actual

monthly peak demand (1,635 kVA). That contributed to the actual monthly net cost saving of 18,010 HKD.

Additionally, the identified optimal threshold based on the non-greedy scheme would, to some extent, be affected by the load prediction accuracy. When the average prediction error went up, the non- greedy adaptive threshold without considering the previous peak power use would also increase, and vice versa. But, due to considering the previous peak power use in updating the monthly threshold, the slight inaccuracy of load prediction would have little impact on the monthly peak reduction.

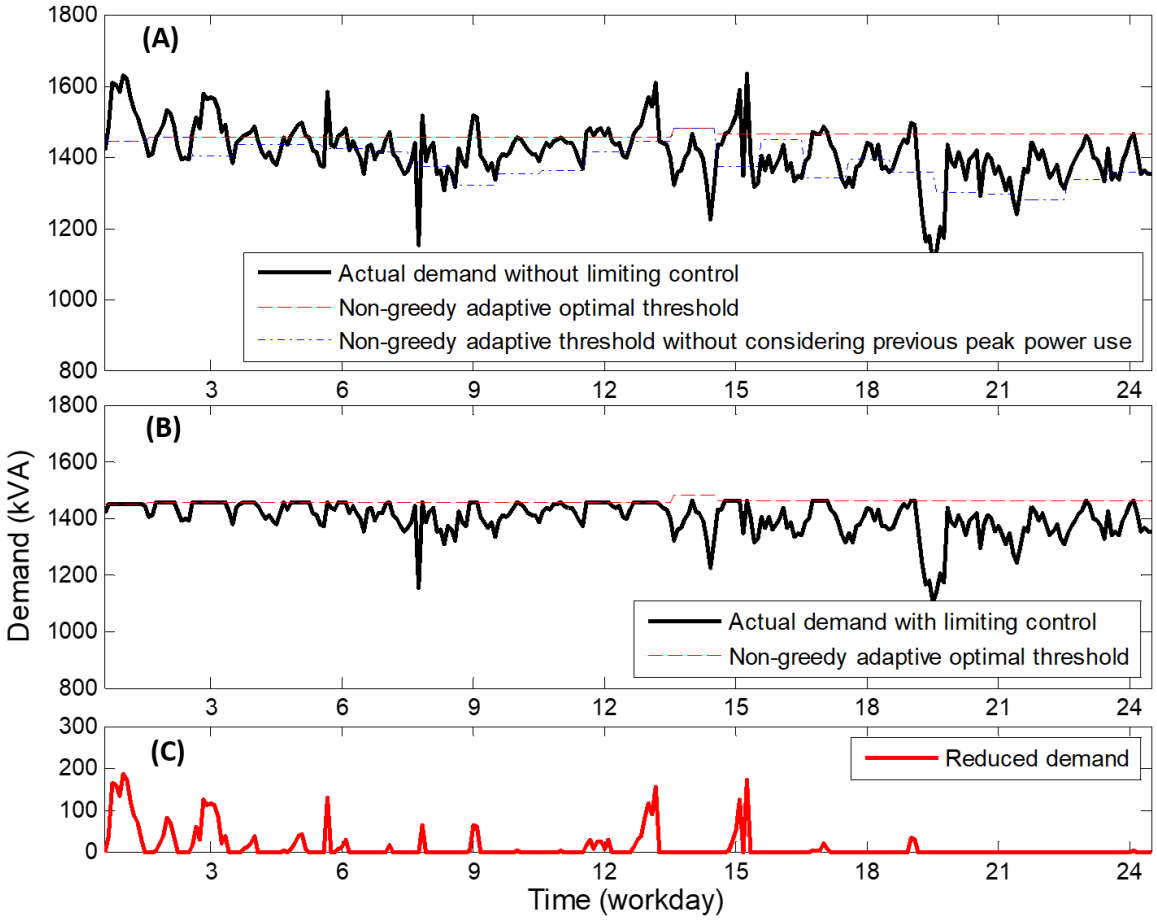


Fig. 7. Building demand profiles in Dec/2017 under different situations: (A) no demand limiting; (B) demand limiting based on the non-greedy scheme; (C) Actual demand reduction based on the non-greedy scheme.

*4.2.2. Validation of greedy scheme*

In validation of the greedy scheme, the updated ever-changing actual power uses are used to identify/update the optimal limiting threshold according to equations (5-6).

Fig. 8(A), identical to Fig. 7(A), shows the building demand profile of the Hotel ICON building without implementing demand limiting. Two adaptive thresholds are also included: the greedy adaptive optimal threshold, and the other is the greedy adaptive threshold without considering previous peak power use.

Fig. 8(B) shows the power demand profile when implementing demand limiting using the developed demand limiting strategy with the greedy scheme. On the first workday, the greedy adaptive optimal threshold was identified as the average value of the optimal monthly thresholds in the same month of the previous 2 years (i.e., 1,496 kVA). From the second workday, the threshold was identified by conducting cost-benefit analysis of the ever-changing actual power uses (using equations (5-6)) from the first day to the current day and no less than the previous peak power use.

Fig. 8(C) shows the demand reduction when implementing the developed strategy with the greedy scheme. After implementing demand limiting based on the greedy scheme in Dec/2017, the monthly peak demand reduction achieved was 139 kVA (with the accumulated limiting effort of 4,330 kWh), 12.4% of the actual monthly peak demand (1,635 kVA). That contributed to the actual monthly net cost saving of 17,101 HKD.

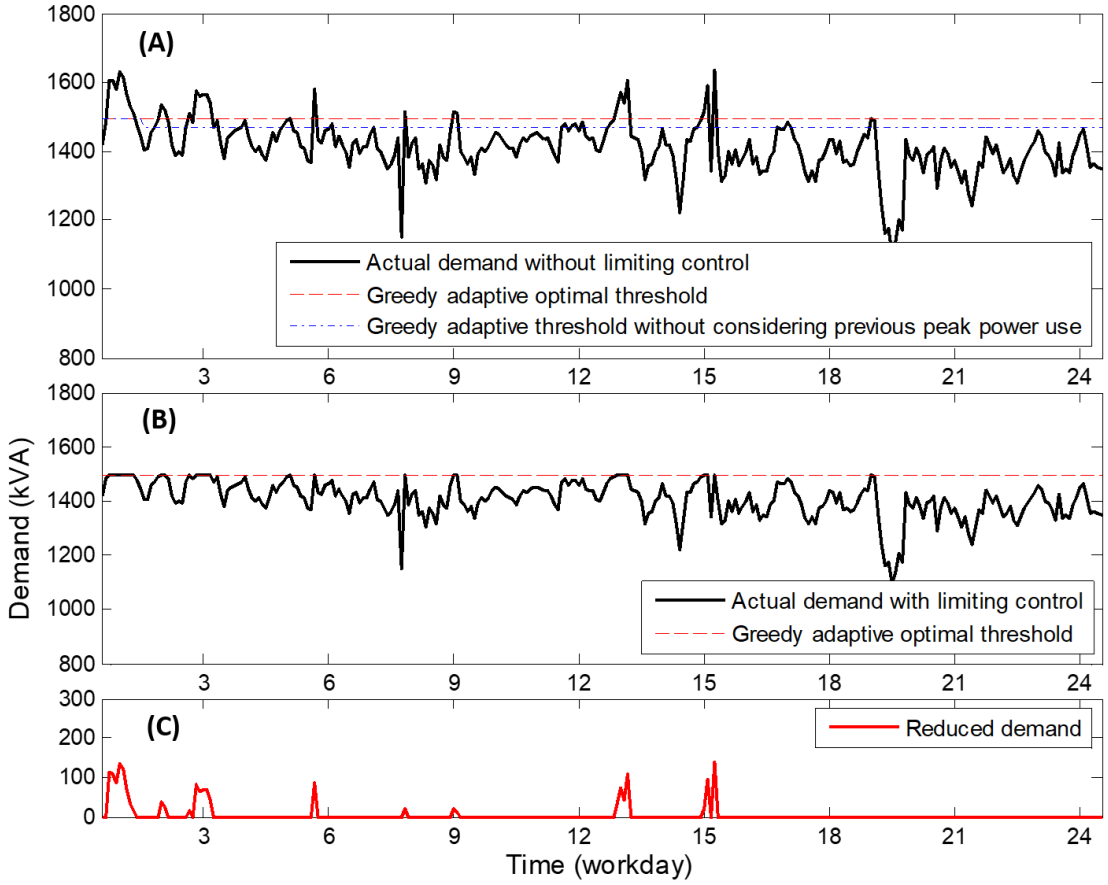


Fig. 8. Building demand profiles in Dec/2017 under different situations: (A) no demand limiting; (B) demand limiting based on the greedy scheme; (C) Actual demand reduction based on the greedy scheme.

*4.2.3. Validation of ε-greedy scheme*

In validation of the ε-greedy scheme, both the updated building demand predictions and the updated ever-changing actual power uses in December are used to identify/update the adaptive optimal limiting threshold. The default value of $\varepsilon$ is set as 0.9.

Fig. 9(A), identical to Fig. 7(A), shows the power demand profile of the Hotel ICON building without implementing demand limiting. Two adaptive thresholds are also included: the ε-greedy adaptive optimal threshold, and the other is the ε-greedy adaptive threshold without considering previous peak power use.

Fig. 9(B) shows the power demand profile when implementing demand limiting using the developed strategy with the ε-greedy scheme. On each workday, the ε-greedy adaptive optimal

threshold was identified as the optimal threshold derived from the greedy scheme with the probability of 90% ($\varepsilon$) or the optimal threshold derived from the non-greedy scheme with the probability of 10%.

Fig. 9(C) shows the demand reduction when implementing the developed strategy with the $\varepsilon$-greedy scheme. After implementing demand limiting based on the $\varepsilon$-greedy scheme in Dec/2017, the monthly peak demand reduction achieved, the accumulated limiting effort of and the actual monthly net cost saving were identical to those according to the greedy scheme.

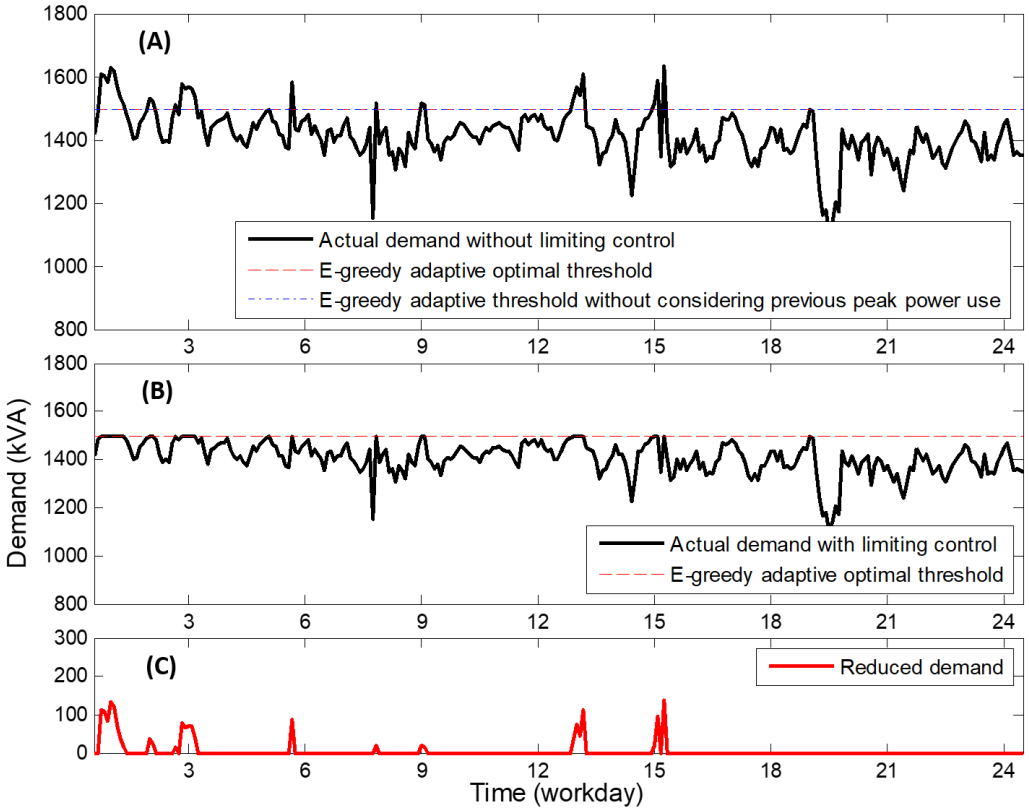


Fig. 9. Building demand profiles in Dec/2017 under different situations: (A) no demand limiting; (B) demand limiting based on the $\varepsilon$-greedy scheme; (C) Actual demand reduction based on the $\varepsilon$-greedy scheme.

In summary, in a typical winter month, demand limiting based on three developed schemes can achieve a significant peak demand reduction. Comparing the non-greedy and greedy schemes, the non-greedy scheme achieved better performance, with 13% more peak demand reduction than that from the greedy scheme. The demand limiting performance (i.e., the monthly peak reduction, the accumulated limiting effort and the monthly net cost saving) based on the $\varepsilon$-greedy scheme were

identical the those using the greedy scheme. This is because the $\varepsilon$-greedy scheme assigned a large weight ($\varepsilon$=0.9) to use the greedy scheme (i.e., exploit ever-changing power uses) to identify the optimal limiting threshold. In this case, there is a high probability for the $\varepsilon$-greedy scheme to obtain the same demand limiting performance as that of the greedy scheme. The uncertainty of demand limiting performance in a winter month when the $\varepsilon$-greedy scheme takes a particular value of $\varepsilon$ is comprehensively analyzed in the later section.

### 4.3. Summer case study and test results

In the summer case study, the datasets during office hours in Jun/2018 are used to validate the adaptive monthly demand limiting strategy using the three proposed schemes.

#### *4.3.1. Validation of non-greedy scheme*

In validation of the non-greedy scheme, the 9-day weather forecast data reported/updated daily by the HKO in June are recorded and used to predict 9-day demand profile on each workday. Afterwards, the daily updated 9-day demand profile is used to identify/update the optimal limiting threshold according to equations (4-5).

Fig. 10(A) shows the power demand profile of the Hotel ICON building without implementing demand limiting, measured in Jun/2018. It can be seen the monthly peak demand occurred on the third workday. Two adaptive thresholds are also included. One is the non-greedy adaptive optimal threshold, and the other is the non-greedy adaptive threshold without considering previous peak power use.

Fig. 10(B) shows the power demand profile when implementing demand limiting using the developed demand limiting strategy with the non-greedy scheme.

Fig. 10(C) shows the demand reduction when implementing the developed strategy with the non-greedy scheme. After implementing demand limiting based on the non-greedy scheme in Jun/2018, the achieved monthly peak demand reduction was 95 kVA (with the accumulated limiting effort of 12,641 kWh), 4.4% of the actual monthly peak demand (2,181 kVA). That contributed to the actual monthly net cost saving of 8,951 HKD.

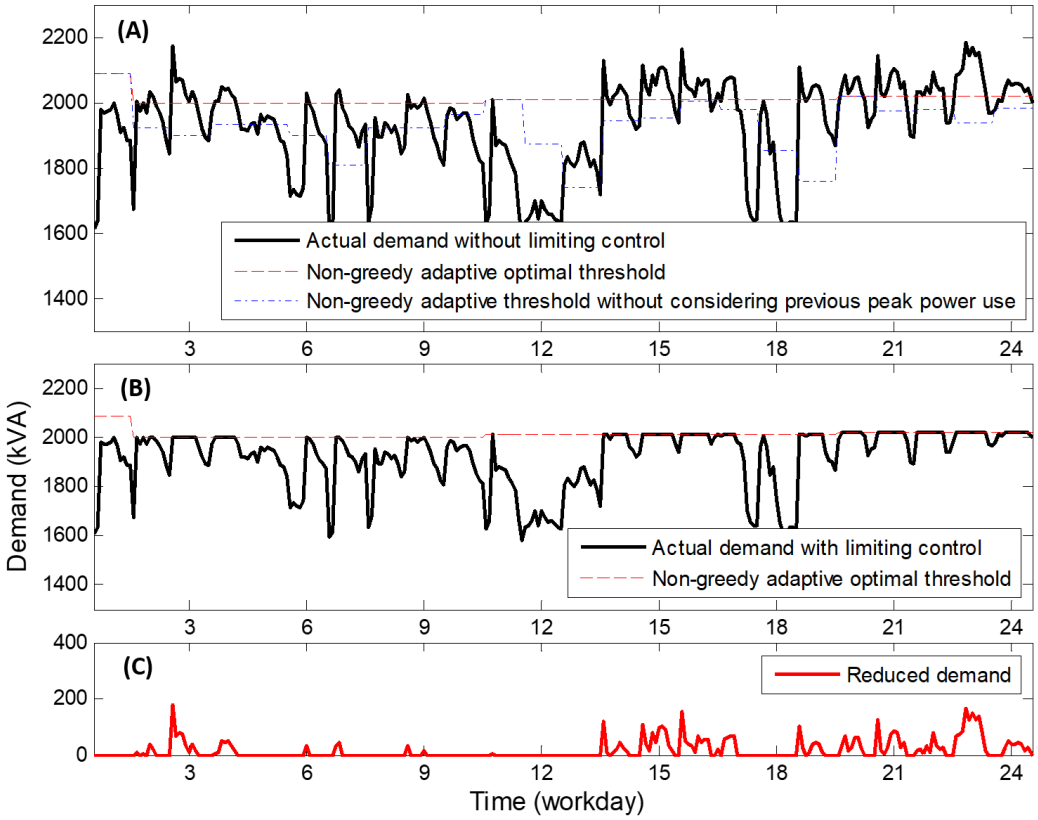


Fig. 10. Building demand profiles in Jun/2018 under different situations: (A) no demand limiting; (B) demand limiting based on the non-greedy scheme; (C) Actual demand reduction based on the non-greedy scheme.

*4.3.2. Validation of greedy scheme*

In validation of the greedy scheme, the updated ever-changing actual power uses are used to identify/update the optimal limiting threshold according to equations (5-6).

Fig. 11(A), identical to Fig. 10(A), shows the power demand profile of the Hotel ICON building without implementing demand limiting.

Fig. 11(B) shows the power demand profile when implementing demand limiting using the developed demand limiting strategy with the greedy scheme. Similarly, on the first workday, the greedy adaptive monthly threshold was determined as the average value of the optimal monthly thresholds in the same month of the previous 2 years (i.e., 2,029 kVA).

Fig. 11(C) shows the demand reduction when implementing the developed strategy with the greedy scheme. After implementing demand limiting based on the greedy scheme in Jun/2018, the

achieved monthly peak demand reduction was 152 kVA (with the accumulated limiting effort of 15,583 kWh), 7.0% of the actual monthly peak demand (2,181 kVA). That contributed to the actual monthly net cost saving of 15,576 HKD.

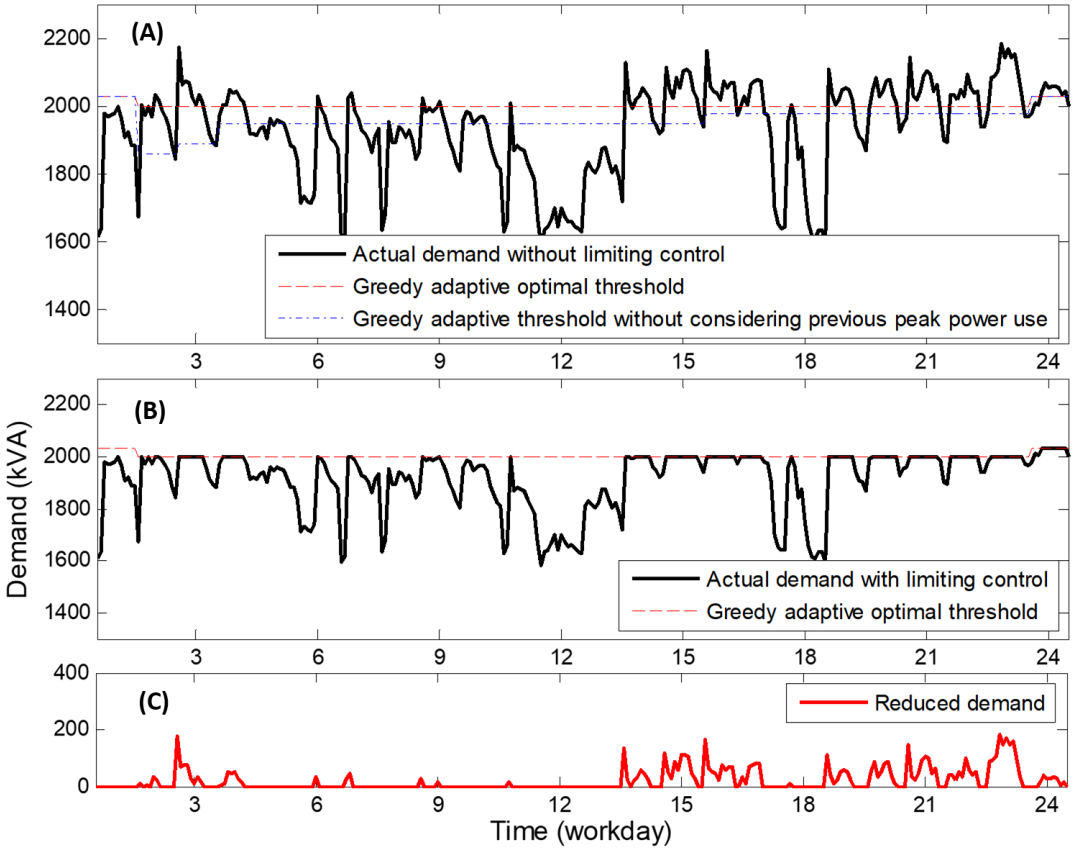


Fig. 11. Building demand profiles in Jun/2018 under different situations: (A) no demand limiting; (B) demand limiting based on the greedy scheme; (C) Actual demand reduction based on the greedy scheme.

*4.3.3. Validation of ε-greedy scheme*

In validation of the $\varepsilon$-greedy scheme, both the updated building demand predictions and the updated ever-changing actual power uses in June are used to identify/update the optimal limiting threshold. The default value of $\varepsilon$ is set as 0.9 as well.

Fig. 12(A), identical to Fig. 10(A), shows the power demand profile of the Hotel ICON building without implementing demand limiting.

Fig. 12(B) shows the power demand profile when implementing demand limiting using the developed demand limiting strategy with the $\varepsilon$-greedy scheme.

Fig. 12(C) shows the demand reduction when implementing the developed strategy with the $\varepsilon$-greedy scheme. After implementing demand limiting based on the $\varepsilon$-greedy scheme in Jun/2018, the achieved monthly peak demand reduction was 152 kVA (with the accumulated limiting effort of 12,426 kWh), 7.0% of the actual monthly peak demand (2,181 kVA). That contributed to the actual monthly net cost saving of 16,485 HKD.

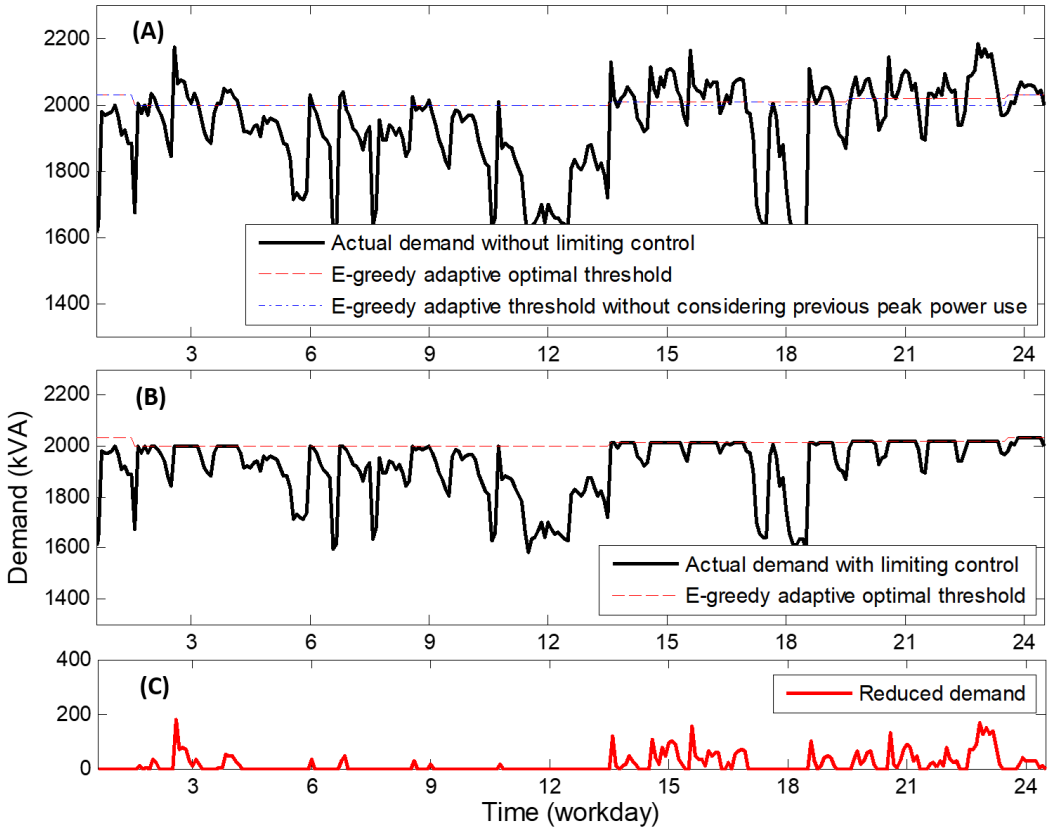


Fig. 12. Building demand profiles in Jun/2018 under different situations: (A) no demand limiting; (B) demand limiting based on the $\varepsilon$-greedy scheme; (C) Actual demand reduction based on the $\varepsilon$-greedy scheme.

In summary, in a typical summer month, demand limiting based on three developed schemes can achieve a satisfactory peak demand reduction. Comparing the non-greedy and greedy schemes, the greedy scheme achieved better performance, with 59% more peak demand reduction than that from the non-greedy scheme. In terms of the $\varepsilon$-greedy scheme, it achieved the same peak demand reduction as the greedy scheme and less accumulated limiting effort than both the non-greedy and greedy schemes. This is also because the $\varepsilon$-greedy scheme assigned a large weight ($\varepsilon$=0.9) to use

the greedy scheme (i.e., exploit ever-changing power uses) to identify the optimal limiting threshold. The uncertainty of demand limiting performance in a summer month when the $\varepsilon$-greedy scheme takes a particular value of $\varepsilon$ is comprehensively analyzed in the following section.

### 4.4. Monte Carlo simulation results

As the $\varepsilon$-greedy scheme uses random sampling to determine the selection of the greedy scheme or non-greedy scheme for threshold resetting on each day, there is great uncertainty in the demand limiting performance over a month. In this case, Monte Carlo simulations of demand limiting based on the $\varepsilon$-greedy scheme are conducted to analyze the uncertainty of demand limiting performance when $\varepsilon$ takes a particular value in both Dec/2017 and Jun/2018. Specifically, under each $\varepsilon$ value ($\varepsilon$ = 0.1, 0.2, …, 0.9), the developed strategy with the $\varepsilon$-greedy scheme is conducted 1000 times.

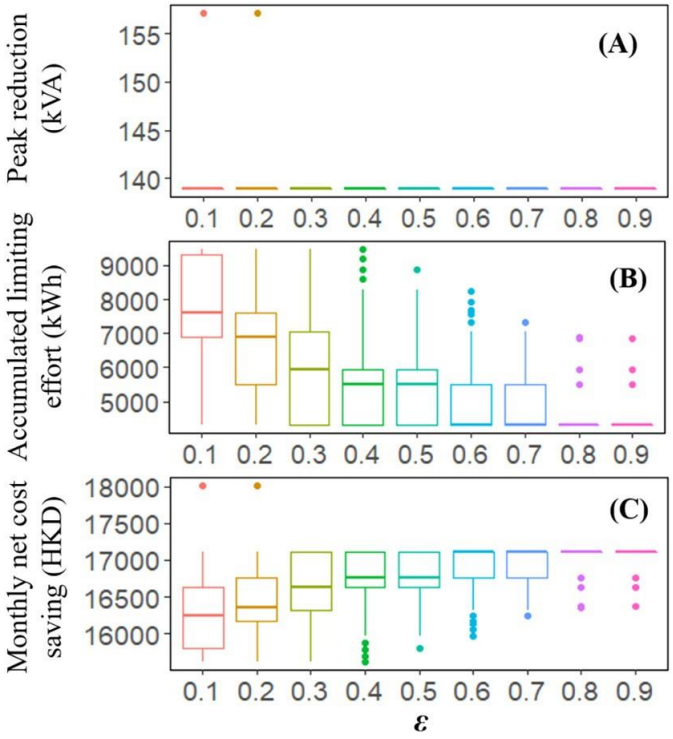


Fig. 13. Boxplot of Monte Carlo simulation results in Dec/2017: (A) peak reduction; (B) accumulated limiting effort; (C) monthly net cost saving.

Fig. 13(A) shows the statistics of the peak demand reduction resulted from the Monte Carlo simulation of demand limiting using the $\varepsilon$-greedy scheme in Dec/2017. It can be seen that, when $\varepsilon$ takes different values, all the 1$^{st}$ quantile, the median and the 3$^{rd}$ quantile of peak demand

reductions are 139 kVA, which is identical to that using the greedy scheme. This is because both the non-greedy and greedy schemes derived a flat limiting threshold and the one from the greedy scheme was larger than that from the greedy scheme. Once the $\varepsilon$-greedy scheme selects the larger limiting threshold from the greedy scheme and meanwhile demand limiting is activated on that day, the monthly limiting threshold from the $\varepsilon$-greedy scheme would be the larger threshold. In this case, there is a high probability for the $\varepsilon$-greedy scheme to select that monthly threshold from the greedy.

Fig. 13(B) shows the statistics of the accumulated demand limiting effort resulted from the Monte Carlo simulation. It can be obviously seen that, with the increase of $\varepsilon$, all the 1$^{st}$ quantile, the median and the 3$^{rd}$ quantile of the accumulated demand limiting efforts decreased and the range between the 1$^{st}$ quantile and the 3$^{rd}$ quantile became smaller. This indicates that the accumulated limiting effort paid for monthly peak demand limiting using the ε-greedy scheme would be larger and more uncertain when $\varepsilon$ takes a smaller value.

Fig. 13(C) shows the statistics of the monthly net cost saving resulted from the Monte Carlo simulation. It can be seen that, with the increase of $\varepsilon$, all the 1$^{st}$ quantile, the median and the 3$^{rd}$ quantile of the monthly net cost savings increased and the range between the 1$^{st}$ quantile and the 3$^{rd}$ quantile became smaller. This indicates that the monthly net cost saving achieved for monthly peak demand limiting using the ε-greedy scheme would be smaller and more uncertain when $\varepsilon$ takes a smaller value.

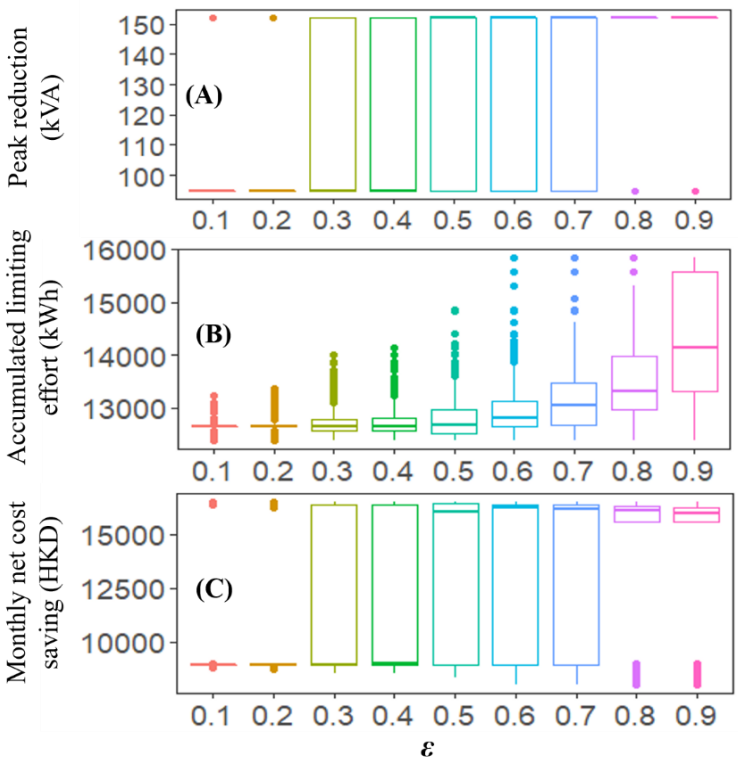


Fig. 14. Boxplot of Monte Carlo simulation results in Jun/2018: (A) peak reduction; (B) accumulated limiting effort; (C) monthly net cost saving.

Fig. 14(A) shows the statistics of the peak demand reduction resulted from the Monte Carlo simulation of demand limiting using the $\varepsilon$-greedy scheme in Jun/2018. It can be seen that the 1st quantile and the median of peak demand reductions are 95 kVA when $\varepsilon \leq 0.4$. When $\varepsilon \geq 0.5$, the median and the 3rd quantile of peak demand reductions are 152 kVA. In other words, the larger $\varepsilon$ is, the higher the probability of achieving a big peak demand reduction is. This is because both the non-greedy and greedy scheme derived the proper monthly threshold in the last few workdays of June. In other words, the monthly threshold from the $\varepsilon$-greedy scheme is mainly determined by $\varepsilon$. When $\varepsilon$ takes a large value, the large weight of the $\varepsilon$-greedy scheme is assigned to use the monthly threshold from the greedy scheme, and vice versa.

Fig. 14(B) shows the statistics of the accumulated demand limiting effort resulted from the Monte Carlo simulation. It can be obviously seen that, with the increase of $\varepsilon$, all the 1st quantile, the median and the 3rd quantile of the accumulated demand limiting efforts increased and the range between the 1st quantile and the 3rd quantile became larger. This indicates that the accumulated limiting effort paid for monthly peak demand limiting using the ε-greedy scheme would be larger

and more uncertain when $\varepsilon$ takes a larger value.

Fig. 14(C) shows the statistics of the monthly net cost saving resulted from the Monte Carlo simulation. It can be seen that, with the increase of $\varepsilon$, the median of the monthly net cost savings increased. Meanwhile, most of monthly net cost savings were equal to particular values with less uncertainty when $\varepsilon$ takes a small or large value (e.g., $\varepsilon = 0.1$ or 0.9).

In comparison of the above Monte Carlo simulation results, the monthly peak demand reduction from the ε-greedy scheme in December was more certain than that in June even when ε took different values ($\varepsilon = 0.1, \ldots, 0.9$). This was mainly due to that in December the greedy scheme derived a flat limiting threshold and was larger than that from the non-greedy scheme, as discussed above. The monthly accumulated limiting effort in these two months was more certain/stable when the ε-greedy scheme assigned the higher prob- ability to select the scheme with the larger threshold (e.g., $\varepsilon = 0.8$ or 0.9 in December, and $\varepsilon = 0.1$ or 0.2 in June). This was because, in the early days of a month, once the ε-greedy scheme selected the larger threshold (from either non-greedy or greedy scheme) and meanwhile demand limiting was activated, the monthly threshold should not be updated to lower values (than the threshold). In this case, the ε-greedy scheme would update the threshold in the same way as the scheme with the larger threshold, and thus the monthly accumulated limiting effort would be relatively certain. As the monthly net cost saving is determined based on the peak demand reduction and the monthly accumulated limiting effort, the changes of net cost savings under different ε values in both December and June were reasonable when considering the changes of peak demand reductions and accumulated limiting efforts in these two months, respectively.

Based on the above case studies, it can be seen that the performances of monthly demand limiting based on the non-greedy scheme are affected by the building load prediction accuracy. The performances of monthly demand limiting based on the greedy scheme can also well achieved by only exploiting the known power uses but are largely affected by the identified threshold on the first day. The ε-greedy scheme is a well hybrid scheme of the above two, which could avoid the worst performance and might obtain the better performance than the non- greedy and greedy schemes. The parameter ε can be flexibly set or altered to update the threshold according to the decision-maker's preference on exploration or exploitation.

## 5. Conclusions

This paper presents an easy-to-use adaptive optimal monthly peak demand limiting strategy based on the exploration and exploitation tradeoff over a month. An ANN-based building load model is developed to predict building demand profiles K days ahead. Three different threshold resetting schemes based on the exploration-exploitation tradeoff are proposed to identify the optimal monthly limiting threshold in an adaptive manner. Monte Carlo simulation is conducted to test the impacts of the exploration-exploitation tradeoff scheme parameter on the demand limiting performance over a month under uncertainties. Based on the case studies and test results, the following conclusions can be made:

- This strategy with either of the proposed threshold resetting schemes can successfully reduce the monthly peak demand and achieve a considerable monthly net cost saving.
- The ANN model for building load prediction is capable of obtaining results with satisfactory accuracy with the average MAPE of 5.7% and the average MAE of 95 kVA.
- In a typical winter month, demand limiting using the three proposed exploration-exploitation tradeoff schemes can achieve a significant monthly peak demand reduction, i.e., 9.6% of the actual monthly peak demand (1,635 kVA) using the non-greedy scheme, and 8.5% of the actual monthly peak demand using both the greedy scheme and $\varepsilon$-greedy scheme ($\varepsilon$ =0.9).
- In a typical summer month, demand limiting using three proposed exploration-exploitation tradeoff schemes can also achieve a satisfactory monthly peak demand reduction, i.e., 4.4% of the actual monthly peak demand (2,181 kVA) using the non-greedy scheme, and 7.0% of the actual monthly peak demand using both the greedy scheme and $\varepsilon$-greedy scheme ($\varepsilon$ =0.9).
- Results of Monte Carlo simulation show that the monthly peak demand reduction from the $\varepsilon$-greedy scheme was more stable when ε takes different values in winter than that in summer. Besides, the monthly accumulated limiting effort in a typical summer or winter month was more certain when the ε-greedy scheme assigned the higher probability for the scheme (either non-greedy or greedy scheme) with the larger threshold.

In summary, this study explores the tradeoff between exploring the predicted building loads and exploiting the actual power uses for adaptive threshold resetting in monthly peak demand limiting. The developed strategy can be widely applied in different regions for that a common format of weather forecasts is applied in the building load model.

**Acknowledgement**

The research presented in this paper is financially supported by a grant (152079/18E) of the Research Grant Council (RGC) of the Hong Kong SAR and a research grant under strategic focus area (SFA) scheme of the research institute of sustainable urban development (RISUD) in The Hong Kong Polytechnic University.

**Appendix A. Identified weight values and bias values in the ANN model training**

Table A.1. Identified weight values and bias values in the ANN model training

| Number | Weight value | | | | | Bias value |
|---|---|---|---|---|---|---|
| | *H* | *D* | *M* | *T* | *RH* | |
| 1 | 1.08 | -0.85 | -1.54 | 0.95 | 1.08 | -2.8311 |
| 2 | 1.53 | 1.47 | -0.99 | 1.25 | 1.53 | -2.0426 |
| 3 | -0.16 | -0.52 | 2.31 | 0.86 | -0.16 | 1.8379 |
| 4 | 1.15 | -0.78 | 1.33 | 1.55 | 1.15 | -1.3999 |
| 5 | 1.09 | 1.60 | 1.06 | -1.31 | 1.09 | -0.5914 |
| 6 | 1.63 | 1.20 | 0.92 | 1.37 | 1.63 | -0.0672 |
| 7 | -0.11 | -0.38 | -2.17 | -1.42 | -0.11 | -0.0962 |
| 8 | -1.67 | -1.77 | 0.46 | -0.71 | -1.67 | -0.4313 |
| 9 | -1.57 | 0.63 | 0.67 | 1.81 | -1.57 | -1.1751 |
| 10 | 1.86 | 0.09 | -0.31 | 1.80 | 1.86 | 1.6565 |
| 11 | -0.14 | 1.78 | 1.80 | -0.72 | -0.14 | -2.0616 |
| 12 | 1.83 | -0.95 | 0.48 | -1.52 | 1.83 | 2.5982 |

*Remark: H, D, M, T, and RH represent input variables of the ANN model.*

**Appendix B. Statistics between load and temperature in July and December**

Fig. B.1 shows the statistics between load and temperature in July in the training (years 2013 to 2015) and test (year 2016) samples. To some extent, the loads in 2016 were relatively lower than those in the training sample at the same temperature.

Fig. B.2 shows the statistics between load and temperature in December in the training (years 2013 to 2015) and test (year 2016) samples. It is evident that the average temperature in 2016 were larger than those in the training data. When temperatures were less than 17 °C or larger than 23 °C, loads in 2016 were relatively lower than those in the training sample at the same temperature. Besides the training data with temperature over 23 °C were much fewer compared to those with

temperature less than 23 °C.

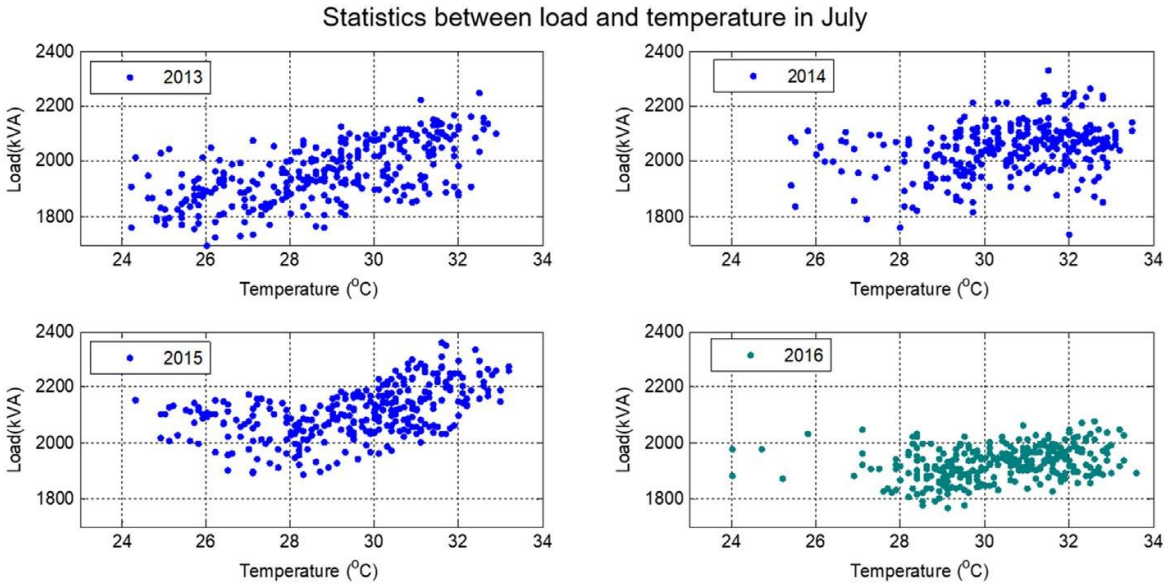


Fig. B.1. Load and temperature in July in the training and test samples.

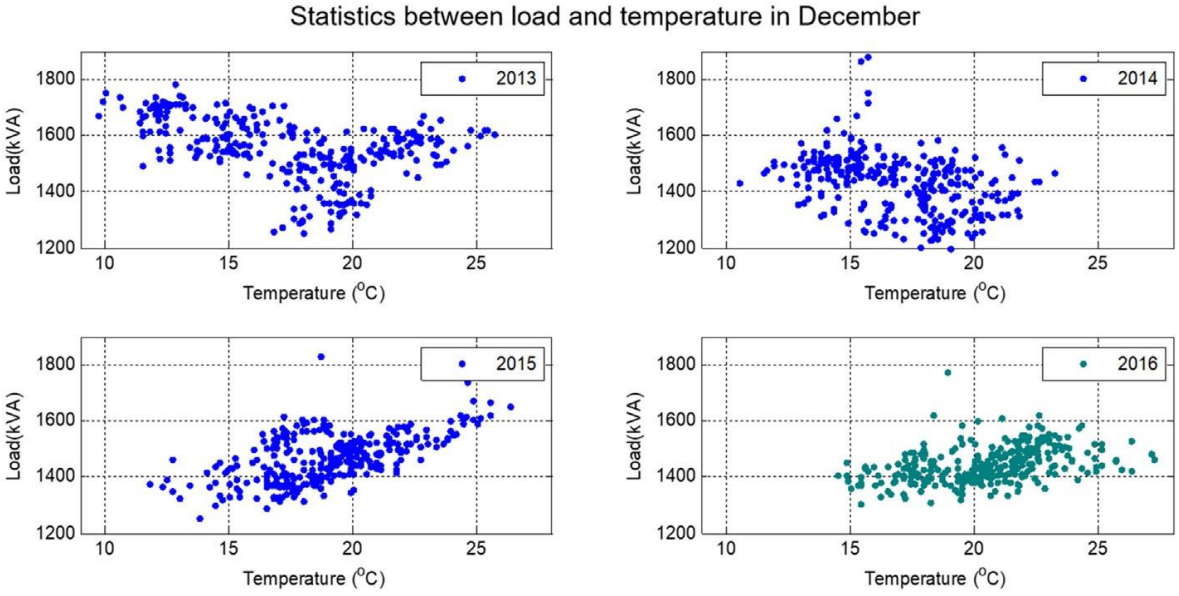


Fig. B.2. Load and temperature in December in the training and test samples.

**References**

[1] D. Ürge-Vorsatz, L. Cabeza, S. Serrano, C. Barreneche, K. Petrichenko, Heating and cooling energy trends and drivers in buildings, Renew. Sust. Energ. Rev. 41 (2015) 85–98, https://doi.org/10.1016/j.rser.2014.08.039.

[2] Electrical and Mechanical Services Department, Hong Kong Energy End-use Data, http://www.emsd.gov.hk/emsd/eng/pee/edata_1.shtml, (2016) (accessed date: 28 Jan 2019).

[3] J. Wells, D. Haas, Electricity Markets: Consumers Could Benefit From Demand Programs, But Challenges Remain, DIANE Publishing, 2004 (ISBN: 0756745802, 9780756745806).

[4] D. Gao, Y. Sun, Y. Lu, A robust demand response control of commercial buildings for smart grid under load prediction uncertainty, Energy 93 (2015) 275–283, https://doi.org/10.1016/j.energy.2015.09.062.

[5] J. Seem, Adaptive demand limiting control using load shedding, HVAC&R Res. 1 (1) (1995) 21–34, https://doi.org/10.1080/10789669.1995.10391306.

[6] Y. Sun, S. Wang, F. Xiao, D. Gao, Peak load shifting control using different cold thermal energy storage facilities in commercial buildings: a review, Energy Convers. Manag. 71 (2013) 101–114, https://doi.org/10.1016/j.enconman.2013.03.026.

[7] L. Shen, Z. Li, Y. Sun, Performance evaluation of conventional demand response at building-group-level under different electricity pricings, Energy Build. 128 (2016) 143–154, https://doi.org/10.1016/j.enbuild.2016.06.082.

[8] P. Xu, P. Haves, M. Piette, L. Zagreus, Demand shifting with thermal mass in large Commercial buildings: field Tests, simulation and audits, Lawrence Berkeley National Laboratory, Available from: https://escholarship.org/content/ qt14j2n3b3/qt14j2n3b3.pdf, (2006) (accessed on 29 Jan 2019).

[9] K. Lee, J. Braun, Development of methods for determining demand-limiting setpoint trajectories in buildings using short-term measurements, Build. Environ. 43 (10) (2008) 1755–1768, https://doi.org/10.1016/j.buildenv.2007.11.004.

[10] G. Henze, C. Felsmann, G. Knabe, Evaluation of optimal control for active and passive building thermal storage, Int. J. Therm. Sci. 43 (2) (2004) 173–183, https://

doi.org/10.1016/j.ijthermalsci.2003.06.001.

[11] K. Drees, J. Braun, Development and evaluation of a rule-based control strategy for ice storage systems, HVAC&R Res. 2 (4) (1996) 312–334, https://doi.org/10.1080/10789669.1996.10391352.

[12] G. Henze, Energy and cost minimal control of active and passive building thermal storage inventory, J. Sol. Energy Eng. 127 (3) (2005) 343–351, https://doi.org/10. 1115/1.1877513.

[13] G. Zhou, M. Krarti, G. Henze, Parametric analysis of active and passive building thermal storage utilization, J. Sol. Eng. 127 (1) (2005) 37–46, https://doi.org/10. 1115/1.1824110.

[14] Y. Sun, S. Wang, G. Huang, A demand limiting strategy for maximizing monthly cost savings of commercial buildings, Energy Build. 42 (11) (2010) 2219–2230, https://doi.org/10.1016/j.enbuild.2010.07.018.

[15] L. Xu, S. Wang, F. Xiao, An adaptive optimal monthly peak building demand limiting strategy considering load uncertainty, Applied Energy 253 (2019) 113582, https://doi.org/10.1016/j.apenergy.2019.113582

[16] Y. Niv, D. Joel, I. Meilijson, E. Ruppin, Evolution of reinforcement learning in uncertain environments: a simple explanation for complex foraging behaviors, Adapt. Behav. (2002), https://doi.org/10.1177/1059-712302-010001-01.

[17] H. Phillips, N. Howai, G. Stan, A. Faisal, The implied exploration-exploitation trade-off in human motor learning, BMC Neuroscience 12 (1) (2011) 98, https://doi.org/ 10.1186/1471-2202-12-S1-P98.

[18] P. Auer, N. Cesa-Bianchi, P. Fischer, Finite-time analysis of the multiarmed bandit problem, Mach. Learn. 47 (2–3) (2002) 235–256, https://doi.org/10.1023/ A:1013689704352.

[19] G. Zhang, B. Patuwo, M. Hu, Forecasting with artificial neural networks: the state of the art, Int. J. Forecast. 14 (1) (1998) 35–62, https://doi.org/10.1016/S01692070(97)00044-7.

[20] M. Cilimkovic, Neural networks and back propagation algorithm, 15 Institute of Technology Blanchardstown, Blanchardstown Road North Dublin, 2015 Available from http://dataminingmasters.com/uploads/studentProjects/NeuralNetworks.pdf (accessed on 29 Jan 2019).

[21] M. Benedetti, V. Cesarotti, V. Introna, J. Serranti, Energy consumption control automation

using Artificial Neural Networks and adaptive algorithms: proposal of a new methodology and case study, Appl. Energy 165 (2016) 60–71, https://doi.org/ 10.1016/j.apenergy.2015.12.066.

[22] S. Kalogirou, Artificial neural networks in renewable energy systems applications: a review, Renew. Sust. Energ. Rev. 5 (4) (2001) 373–401, https://doi.org/10.1016/ S1364-0321(01)00006-5.

[23] D. Rumelhart, G. Hinton, R. Williams, Learning internal representations by error propagation, California Univ San Diego La Jolla Inst for Cognitive Science, 1985 Available from https://apps.dtic.mil/dtic/tr/fulltext/u2/a164453.pdf (accessed on Jan 30 2019).

[24] S. Wang, X. Xu, Simplified building model for transient thermal performance estimation using GA-based parameter identification, Int. J. Therm. Sci. 45 (4) (2006) 419–432, https://doi.org/10.1016/j.ijthermalsci.2005.06.009.

[25] C. Yan, S. Wang, C. Fan, F. Xiao, Retrofitting building fire service water tanks as chilled water storage for power demand limiting, Build. Serv. Eng. Res. Technol. 38 (1) (2017) 47–63, https://doi.org/10.1177/0143624416669553.

[26] B. Cui, S. Wang, Y. Sun, Life-cycle cost benefit analysis and optimal design of small scale active storage system for building demand limiting, Energy 73 (2014) 787–800, https://doi.org/10.1016/j.energy.2014.06.084.